Available online at www.sciencedirect.com
ScienceDirect
ELSEVIER
ISPRS Journal of Photogrammetry & Remote Sensing 62 (2007) 201–216
PHOTOGRAMMETRY & REMOTE SENSING
www.elsevier.com/locate/isprsjprs

Scaling functions for landscape pattern metrics derived from remotely sensed data: Are their subpixel estimates really accurate?

Santiago Saura *, Sandra Castro

University of Lleida. ETSEA. Department of Agroforestry Engineering. Av. Rovira Roure, 191. 25198, Lleida, Spain

Received 29 November 2006; received in revised form 13 March 2007; accepted 14 March 2007
Available online 25 April 2007

Abstract

One of the most rapidly growing applications of remotely sensed data is the derivation of landscape pattern metrics for the assessment of land cover condition and landscape change dynamics. The availability of a wide variety of sensors allows for characterisation of land cover at multiple spatial scales, and increases the need for practical scaling techniques that permit the comparison of pattern estimates across different spatial resolutions. Previous research has reported on scaling functions describing the variations of different landscape pattern metrics with spatial resolution; this may be particularly useful in downscaling spatial pattern characteristics, but no quantitative results or independent validation have been reported yet in this respect. We analysed a wide set of landscape data derived from remotely sensed images covering different study areas, sensor spatial resolutions, and classification approaches (pixel-based and object-based), which were aggregated to coarser resolutions through majority filters. We considered eight landscape pattern metrics for which predictable scaling functions have been reported, and compared the subpixel estimates provided by those scaling functions (when fitted to the metric values for different ranges of spatial resolution above the pixel level) with the true value of the metric at the subpixel resolution. We found that for metrics like mean patch size, landscape shape index or edge length, quite accurate subpixel estimates were achieved in all the datasets, even for relatively large downscaling factors. However, the opposite was the case for several of the metrics for which a predictable scaling behaviour had been previously described. The most accurate subpixel estimates were obtained when only a narrow range of spatial resolutions (closest to the subpixel resolution) was used to fit the scaling function, suggesting that the scaling functions are not fully scale invariant. We also found that the performance of available scaling functions is much lower in object-based data (in comparison with per-pixel classified data) for ranges of spatial resolution below the characteristic minimum mapping unit of the interpreted or segmented image. We conclude that scaling functions may be useful and reasonably accurate for estimating pattern metrics at the subpixel level, but only if the specific scaling recommendations and limitations reported in this study are taken into account.

Keywords: Scale; Landscape pattern; Sensor spatial resolution; Spatial metrics; Landscape ecology; Land cover analysis

1. Introduction

One of the most rapidly growing applications of remotely sensed data is the derivation of landscape pattern

* Corresponding author. Tel.: +34 973 702877; fax: +34 973 702673.
E-mail address: ssaura@eagrof.udl.es (S. Saura).
URL: http://www.udl.es/usuaris/saura (S. Saura).

0924-2716/$ - see front matter © 2007 International Society for Photogrammetry and Remote Sensing, Inc. (ISPRS). Published by Elsevier B.V. All rights reserved.
doi:10.1016/j.isprsjprs.2007.03.004

metrics for the assessment of land cover condition and landscape change dynamics (Betts et al., 2003; Colombo et al., 2004; Egbert et al., 2002; Griffith et al., 2003; Hansen et al., 2001; Imbernon and Branthomme, 2001; Jorge and García, 1997; Millington et al., 2003; Peralta and Mather, 2000; Sader et al., 2003; Sachs et al., 1998; Skole and Tucker, 1993; Vogelmann, 1995; Yu and Ng, 2006). This is due to the increasing awareness of the effects of the spatial arrangement of ecosystems on different ecological processes (spread of forest fires and other disturbances, species richness distribution, movement and persistence of animal populations, water flows, etc.), all of them relevant for the maintenance of biodiversity (e.g. Forman, 1995; Turner, 1989). The quantification and monitoring of spatial patterns at the landscape scale is made possible by the analysis of satellite images, which provide the necessary information in a digital format over large areas in a cost effective manner.

Satellite images with various spatial resolutions are used as the primary source of information for the analysis of landscape patterns. The availability of a wide variety of sensors allows for the characterisation of land cover at multiple spatial scales; moreover, a multi-scale assessment has been recommended in order to adequately characterise and monitor landscape patterns, since both pattern and process in ecological systems often operate on multiple scales (Wu, 2004). In this context, there is an urgent need of practical scaling techniques that allow for comparing and transferring pattern estimates across different spatial resolutions (Saura, 2004).

Numerous studies have analysed the effect of spatial resolution on landscape pattern metrics (Benson and MacKenzie, 1995; Frohn, 1998; Frohn and Hao, 2006; Frohn et al., 1996; García-Gigorro and Saura, 2005; Hlavka and Livingston, 1997; Kojima et al., 2006; Millington et al., 2003; Saura, 2001, 2004; Turner et al., 1989; Wickham and Riitters, 1995; Wu et al., 2000, 2002; Wu, 2004). It is well known that there are large differences in the values of the fragmentation indices derived from satellite images with different spatial resolutions, and the general trends of the variations of these metrics with spatial resolution have been characterised. Different authors have experimentally found that the variation of several landscape pattern metrics with spatial resolution can be described through scaling functions such as power laws (Frohn, 1998; Frohn and Hao, 2006; Saura, 2001, 2004; Wu et al., 2002; Wu, 2004). Considering the apparent good fit of these scaling functions to a wide set of landscape data, it has been suggested that the extrapolation and interpolation of these metrics across different pixel sizes can be done simply and accurately (Wu et al., 2002; Wu, 2004). However, Saura (2004) noted that the coefficients of the scaling functions (which are needed for the scaling process itself) cannot be known *a priori* for a certain image or landscape, rather they have to be determined empirically by previously fitting the scaling function to a set of metric values computed on the aggregated image at different spatial resolutions. For this reason, scaling functions seem to be of little aid for upscaling pattern estimates (i.e. obtaining metric values at coarser spatial resolutions), since in fact they require as an input those metric values at broader pixel sizes. The major interest of these scaling functions may be estimating pattern metrics at the subpixel level (i.e., at a spatial resolution finer than the original pixel size of the image). In fact, this may represent the only operational procedure to downscale spatial pattern characteristics (Saura, 2004), although no quantitative results have been provided yet, apart from a single forest class and range of spatial resolutions by García-Gigorro and Saura (2005), who found poor results with the use of scaling functions for downscaling three fragmentation metrics. As noted by García-Gigorro and Saura (2005), the downscaling problem may be much more complicated than the upscaling one, since it implies predicting a metric value corresponding to a fine spatial resolution that is not available in existing data and that in principle cannot be recreated by combining the information existing in coarse-scale data (but see Tatem et al., 2002).

Indeed, most of the previous research has not gone beyond a descriptive analysis of scale effects on pattern metrics. In this study, we intend to go further by quantitatively assessing and validating the true accuracy and utility of available scaling functions for obtaining subpixel estimates of pattern metrics, by analysing a broad set of landscape data derived from remotely sensed data covering different study areas, sensor spatial resolutions, and classification approaches. Specifically, we perform an independent validation of these functions by fitting them to different ranges of spatial resolution (always broader than the subpixel resolution to be estimated), and comparing the subpixel estimates obtained through the scaling functions with the true value of the pattern metrics at that resolution. We analyse how the accuracy of subpixel pattern estimates varies for different metrics, ranges of spatial resolution used to estimate the scaling behaviour, downscaling factors, and classification approaches adopted to extract the pattern information from the remotely sensed data. Finally, we provide recommendations for the adequate use of scaling functions for downscaling landscape pattern characteristics.

2. Methods

2.1. Spatial data

We analysed the following four different land cover datasets (Fig. 1) derived from remotely sensed images covering four study areas with different sensor spatial resolutions and classification approaches commonly used for landscape pattern analysis:

– A (Fig. 1). A 4000×4000 pixel subset of the Global Land Cover (GLC) Characteristics Database (version 1.2) for Eurasia, developed by the U.S. Geological Survey (USGS), the University of Nebraska—Lincoln, and the European Commission's Joint Research Centre. This is a 1-km resolution dataset based on multi-temporal unsupervised per-pixel classification of Advanced Very High Resolution Radiometer (AVHRR) data (spanning April 1992 through March 1993), with post-classification refinement using multi-source earth data (Loveland et al., 2000). This database is available at http://edcsns17.cr.usgs.gov/glcc/. The USGS Land Use/Land Cover System Legend differentiates up to 24 land cover classes. The most abundant land cover classes in the analysed subset were grassland, shrubland, barren or sparsely vegetated, mixed forest, deciduous needleleaf forest, dryland cropland and pasture, and wooded tundra.

– B (Fig. 1). A 4000×4000 pixel subset of the USGS National Land Cover (NLC) Dataset 1992 for Oregon, USA. This dataset comprises 21 different classes and has a spatial resolution of 30×30 m. It

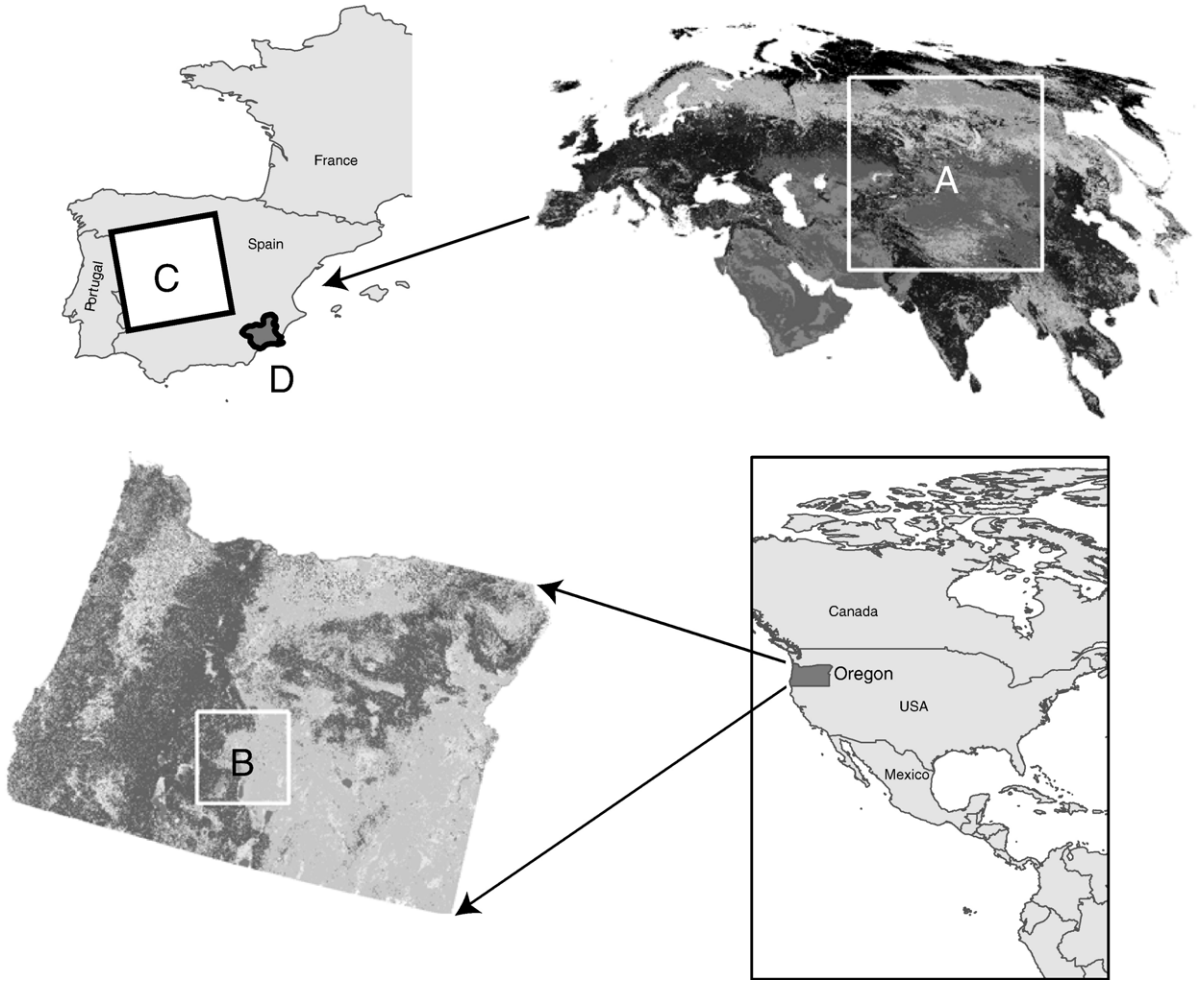

Fig. 1. Location of the four analysed datasets. A) Subset of the Global Land Cover Characteristics (GLC) Database for Eurasia (upper right). B) Subset of the USGS National Land Cover (NLC) Dataset for Oregon (bottom left). C) Subset of the CORINE European Land Cover Database for Spain (upper left). D) Spanish Forest Map (SFM) for the region of Murcia (upper left, SE Spain).

has been derived from the per-pixel classification of Landsat Thematic Mapper (TM) data through an unsupervised clustering algorithm, with the resulting clusters refined and labelled using aerial photography, ground observations, and various ancillary data (Vogelmann et al., 1998a,b). This dataset is available at http://edc.usgs.gov/products/landcover/nlcd.html. The most abundant land cover classes in the analysed subset were shrubland, evergreen forest, grasslands/herbaceous, bare rock/sand/clay, emergent herbaceous wetlands, pasture/hay, and open water.

– C (Fig. 1). A 4000×4000 pixel subset of the CORINE European Land Cover Database (Commission of the European Communities, 1993) for Spain. This dataset is derived from the interpretation of satellite images (Landsat TM, Landsat MSS, Spot XS) and ancillary data (Commission of the European Communities, 1993). It has a hierarchical legend with 44 land cover classes, a minimum mapping unit of 25 ha, and is distributed as a raster dataset with a spatial resolution of 100×100 m. The most abundant land cover classes in the analysed subset were non-irrigated arable land, sclerophyllous vegetation, natural grassland, agro-forestry areas, broad-leaved forest, transitional woodland-scrub, complex cultivation patterns, and coniferous forest.

– D (Fig. 1). Spanish Forest Map (SFM) for the region of Murcia (3077×2998 pixels), developed in coordination with the Third Spanish National Forest Inventory (Ministerio de Medio Ambiente, 2002). The SFM was obtained from the interpretation of aerial photographs, combined with pre-existing maps and field inventory data. The minimum mapping unit is typically 6.25 ha, decreasing to 2.2 ha in the case of forest patches embedded in a non-forest land use matrix. Land cover is classified into 35 categories including both forest and non-forest types. This map is analysed in raster format with a spatial resolution of 50×50 m for the characterisation of forest landscape structure and configuration within the Third Spanish National Forest Inventory (Ministerio de Medio Ambiente, 2002). The most abundant land cover classes in Murcia are agricultural lands, natural forest, grassland, plantation forest, and artificial areas.

Two of these datasets were obtained through per-pixel classifiers (GLC, NLC), while the other two (CORINE, SFM) were derived as object-based classifications from the interpretation of remotely sensed images by human analysts. The scale of the GLC and NLC is characterised by the pixel size or spatial resolution of the satellite images, while in the CORINE and SFM the degree of spatial detail is determined by the size of the minimum mapping unit (MMU, which is much larger than the pixel size of the interpreted image). Object-based classifications can be obtained either through image interpretation or through segmentation algorithms applied to remotely sensed data. This results in a partition of the image into spatially continuous, non-intersecting and homogeneous (according to certain criteria) regions or objects (Desclée et al., 2006; Hay et al., 2003; Pal and Pal, 1993). Instead of analysing single pixels independently of their location, similar contiguous pixels are grouped into objects, which allows for the incorporation of valuable information contained in the relationships between adjacent pixels, including texture, context and shape (Benz et al., 2004; Desclée et al., 2006; Laliberte et al., 2004; Walter, 2004).

The datasets were aggregated into coarser spatial resolutions through majority filters (as in Benson and MacKenzie, 1995; Frohn, 1998; Saura, 2001; Turner et al., 1989; Wickham and Riitters, 1995; Wu et al., 2002; Wu, 2004) applied to the original images (in windows of 3×3, 5×5, 7×7, 9×9 pixels, etc.), up to where the aggregated images resulted in a minimum of 100×100 pixels, as in Wu et al. (2002) and Wu (2004). This resulted in a maximum aggregation corresponding to a 39×39 filter for GLC, NLC and CORINE datasets and to a 31×31 filter for the SFM. Only land cover classes sufficiently abundant to remain present in the images for a wide range of spatial resolutions after aggregation were included in subsequent analysis. This resulted in 61 classes for the four datasets, and a total of 1188 values for each pattern metric (for the different classes and aggregations).

2.2. Pattern metrics

We analysed the scaling behaviour of eight landscape pattern metrics for which a stable and predictable scaling function has been reported in previous studies (Frohn, 1998; Frohn and Hao, 2006; Saura, 2001, 2004; Wu et al., 2002; Wu, 2004), and particularly in Wu (2004). Some metrics were not considered because essentially they quantified the same information as the metrics that were already included. For example, patch density and edge density were not analysed because they were redundant with number of patches and edge length, since the extent is kept constant while varying the spatial resolution. All the metrics were computed at the class level (i.e. a single metric value summarising the spatial characteristics of all the patches within a certain land cover class), both on the

original and aggregated images through the Fragstats 3.3 software (McGarigal et al., 2002). Further details on the ecological implications of these pattern characteristics can be found in Forman (1995). The eight analysed metrics are:

1. Number of patches (NP), where a patch is defined by the 8-neighbourhood rule (set of pixels belonging to the same class and sharing one of their sides or vertices), with a higher NP indicating greater fragmentation.
2. Mean Patch Size (MPS), a simple and common fragmentation metric, with a lower MPS indicating greater fragmentation.
3. Patch Size Standard Deviation (PSSD).
4. Largest Patch Index (LPI), defined as the percent of total image area occupied by the largest sized patch of the class of interest.
5. Edge length (EL), where an edge is defined as any side shared between two pixels belonging to different classes (one of them being the class under analysis). EL is regarded as a good indicator of pattern fragmentation, with more fragmented patterns yielding a higher EL.
6. Landscape shape index (LSI), computed as the total class perimeter divided by the minimum perimeter possible for a maximally aggregated class, which is achieved when the class is maximally clumped into a single, compact patch (McGarigal et al., 2002). Despite the name given to this metric, LSI does not really measure pattern shape, but is more related to the degree of pattern fragmentation (Saura and Carballal, 2004), and conveys the same information as the aggregation index by He et al. (2000).
7. Area-weighted mean shape index (AWMSI), computed as an area-weighted mean of the shape index for each patch in the analysed class, where the shape index equals the patch perimeter divided by the minimum perimeter possible for a maximally compact shape (in a square raster format) of the same area as the analysed patch (McGarigal et al., 2002). AWMSI is a measure of shape irregularity and increases (with no theoretical upper limit) for more complex or elongated shapes (Saura and Carballal, 2004), attaining its minimum (AWMSI = 1) when all the class patches are maximally compact.
8. Area-weighed mean patch fractal dimension (AWMFD), computed as an area-weighted mean of the fractal dimension index for each patch in the analysed class, where the patch fractal dimension equals two times the logarithm of patch perimeter (where the perimeter is divided by four to correct for the raster bias in perimeter) divided by the logarithm of patch area (McGarigal et al., 2002). AWMFD attains its minimum value (AWMFD = 1) for compact shapes and, as with the AWMSI, increases for more complex or elongated shapes (Kojima et al., 2006; Saura and Carballal, 2004).

2.3. Scaling functions and accuracy testing

The variation with spatial resolution of six of the described class-level metrics has been shown to follow a power law (Eq. (1)) (Wu, 2004), either increasing (MPS) or decreasing (NP, EL, LSI, AWMSI, AWMFD), while for the other two the appropriate scaling function is an increasing linear (PSSD, Eq. (2)) and logarithmic function (LPI, Eq. (3)) (Wu, 2004), as follows:

$$y = a \cdot x^b \tag{1}$$

$$y = a \cdot x + b \tag{2}$$

$$y = a \cdot \ln x + b \tag{3}$$

where y is the metric value corresponding to a spatial resolution of x (length of the pixel side), and a and b are constants that characterise the metric scaling behaviour. The most appropriate scaling function for each metric (Wu, 2004) was fitted to the metric values at different spatial resolutions through least-squares linear regression (as in previous studies on this topic), which corresponds to Eq. (2) for PSSD, Eq. (3) for LPI and to a double-logarithmic linear transformation of the power law (Eq. (1)) for the rest of the metrics.

We fitted the scaling functions to different sets of metric values corresponding to different ranges of spatial resolution (obtained from the aggregated data described earlier). The target resolution (i.e., the spatial resolution at which the pattern metric value is to be estimated through the scaling functions) was always finer than the spatial resolutions used to fit those scaling functions. The target resolution was in most cases the original (finest) spatial resolution of each dataset (1000 m for GLC, 100 m for CORINE, 50 m for SFM and 30 m for NLC), although bigger pixel sizes were also considered, as will be shown later. Comparison of the true value of the pattern metrics at the target resolution with those obtained at that resolution through the scaling functions allowed us to assess and validate the accuracy of the subpixel estimates (pattern metric values estimated at a finer resolution than the finest used to fit the scaling function). The number of data points (metric values for different spatial resolutions) used to fit the

power law was varied to assess how this may influence the resultant subpixel estimates. Obviously, a minimum of two data points was required to determine the two parameters in the scaling functions (Eqs. (1), (2), and (3)) (e.g. metric values at 300 and 500 m to fit the scaling function and estimate the metric value at the 100 m target for the CORINE dataset).

The downscaling performance of the scaling functions was quantified through the accuracy improvement percentage (AI), theoretically ranging from −100 to 100, and computed as:

$$\mathrm{AI}(\%) = 100\frac{|Y_{\mathrm{fin}} - Y_{\mathrm{act}}| - |Y_{\mathrm{est}} - Y_{\mathrm{act}}|}{|Y_{\mathrm{fin}} - Y_{\mathrm{act}}| + |Y_{\mathrm{est}} - Y_{\mathrm{act}}|} \quad (4)$$

where Y_{act} is the actual value of the pattern metric at the target resolution (directly computed on actual spatial data at that spatial resolution, and not estimated through the scaling function), Y_{est} is the pattern metric value at the target resolution estimated through the scaling function and Y_{fin} is the actual pattern metric value in the finest spatial resolution used to fit the scaling function for the downscaling process (this finest resolution is always coarser than the target resolution). When the scaling function provides a perfectly accurate subpixel estimate ($Y_{\mathrm{est}} = Y_{\mathrm{act}}$) then AI = 100%. If $Y_{\mathrm{fin}} = Y_{\mathrm{est}}$ then the scaling function has not contributed to any improvement in the downscaling procedure (and then AI = 0%); simply taking as the subpixel estimate the metric value corresponding to the finest available resolution (the finest resolution that was used to fit the power law) would provide the same result without need for any scaling function. Negative AI values will be obtained when the scaling function estimate is less accurate than just using the metric value at the finest available resolution as the subpixel estimate, a case in which the use of a scaling function should be avoided. Quantifying the downscaling accuracy through AI (instead of other simpler measures such as the standard deviation between Y_{act} and Y_{est}) is particularly important and necessary in this context to take into account the different ranges of variation that each metric has in reality. These can be quite different depending on the analysed metric and often much narrower than its theoretical range of variation (Kojima et al., 2006; Saura and Martínez-Millán, 2001; Saura, 2002). For example, the subpixel estimate for a metric with a low variability in actual landscape patterns may, by being close to the actual target value (low relative error), provide a false impression of accuracy. In fact, any metric value at any resolution may be close to the actual target value, and by simply taking Y_{fin} as the subpixel estimate the result may be more accurate.

3. Results and discussion

3.1. Pixel-based versus object-based classified remotely sensed images

We found that in general subpixel estimates were much more accurate for the GLC and NLC datasets (per-pixel classifications of remotely sensed data) than for the CORINE and SFM images (object-based classifications derived from image interpretation) when the target resolution was at the finest scale for which those data were available (Figs. 2 and 3). For example, the accuracy improvement (AI) for MPS was about 80% for GLC and NLC data (Fig. 2), while it was only about 20% and −70% for SFM and CORINE data, respectively (Fig. 3). Similar results were obtained for most of the pattern metrics.

These results were obtained for a target resolution much below the size of the objects (minimum mapping unit, MMU) characteristic of the CORINE and SFM data (Fig. 3), with an MMU of 25 ha and 6.25 ha, respectively, which is equivalent to a pixel size of about 500 m and 250 m. When spatial resolution is varied below the size of the classified objects, variations of many pattern metrics are much lower than when pixel sizes increase above the MMU (see Fig. 4 for the NP and EL and its comparison with pixel-based data). In an extreme case, the effect would be the same as when resampling an image at a spatial resolution below the original pixel size; the spatial resolution (number of pixels) would increase, but the underlying spatial pattern would not present any visible change (García-Gigorro and Saura, 2005). Therefore, the scaling behaviour of pattern metrics may differ considerably in each of these two cases (pixel-based and object-based classifications), and the scaling functions that best describe metrics variation may also be different (Fig. 4). All the scaling functions for landscape pattern metrics reported thus far have been based only on per-pixel classifications of remotely sensed data (Frohn, 1998; Frohn and Hao, 2006; Saura, 2001, 2004; Wu et al., 2002; Wu, 2004), and may not perform well for land cover data derived from the interpretation or segmentation of remotely sensed images, at least when scaling at spatial resolutions below the MMU (Fig. 4). In this latter case, we found a poor performance of available scaling functions, which may even yield negative AI in a considerable number of cases (Fig. 3). However, when the target resolution and ranges of spatial resolutions used for downscaling are clearly above the MMU we obtained much more accurate subpixel estimates for the object-based datasets (Fig. 5), which are very similar to those

reported for the GLC and NLC images (Fig. 2). Throughout the next sections, we focus on analysing the results of the subpixel estimates above the MMU for the CORINE and SFM datasets (Fig. 5).

This is an important issue to consider since many landscape products are obtained from the segmentation or interpretation of remotely sensed images, rather than from pixel-based classifications. Object-based analysis

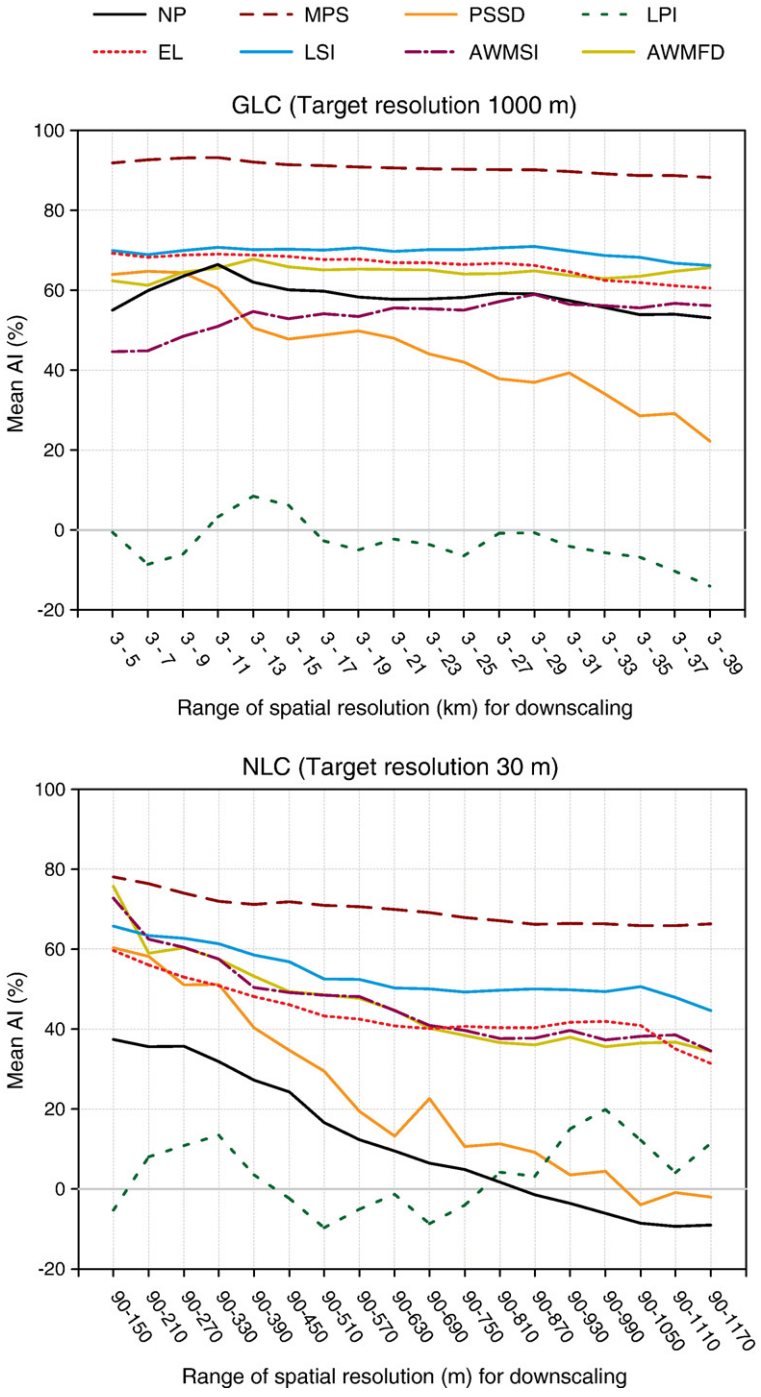

Fig. 2. Mean accuracy improvement (average of the AI values for the different land cover classes in each dataset) of the subpixel estimates for the different pattern metrics and ranges of spatial resolutions used to fit the scaling functions ("range of spatial resolution for downscaling"). Results are shown for the GLC and NLC pixel-based datasets for a target resolution of 1000 m and 30 m, respectively.

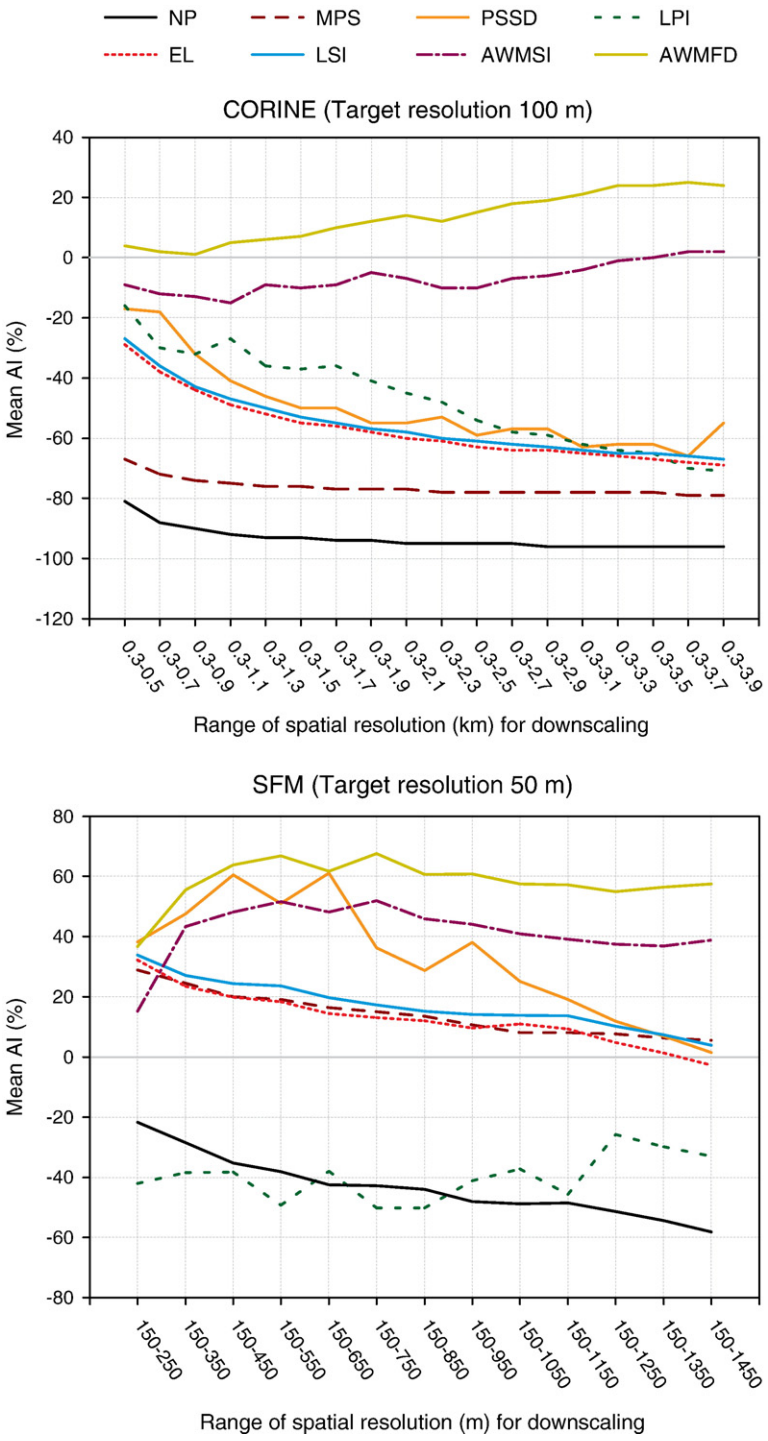

Fig. 3. Mean accuracy improvement (average of the AI values for the different land cover classes in each dataset) of the subpixel estimates for the different pattern metrics and ranges of spatial resolutions used to fit the scaling functions ("range of spatial resolution for downscaling"). Results are shown for the CORINE and SFM object-based datasets for a target resolution (100 and 50 m respectively) below their minimum mapping unit (25 ha and 6.25 ha, respectively).

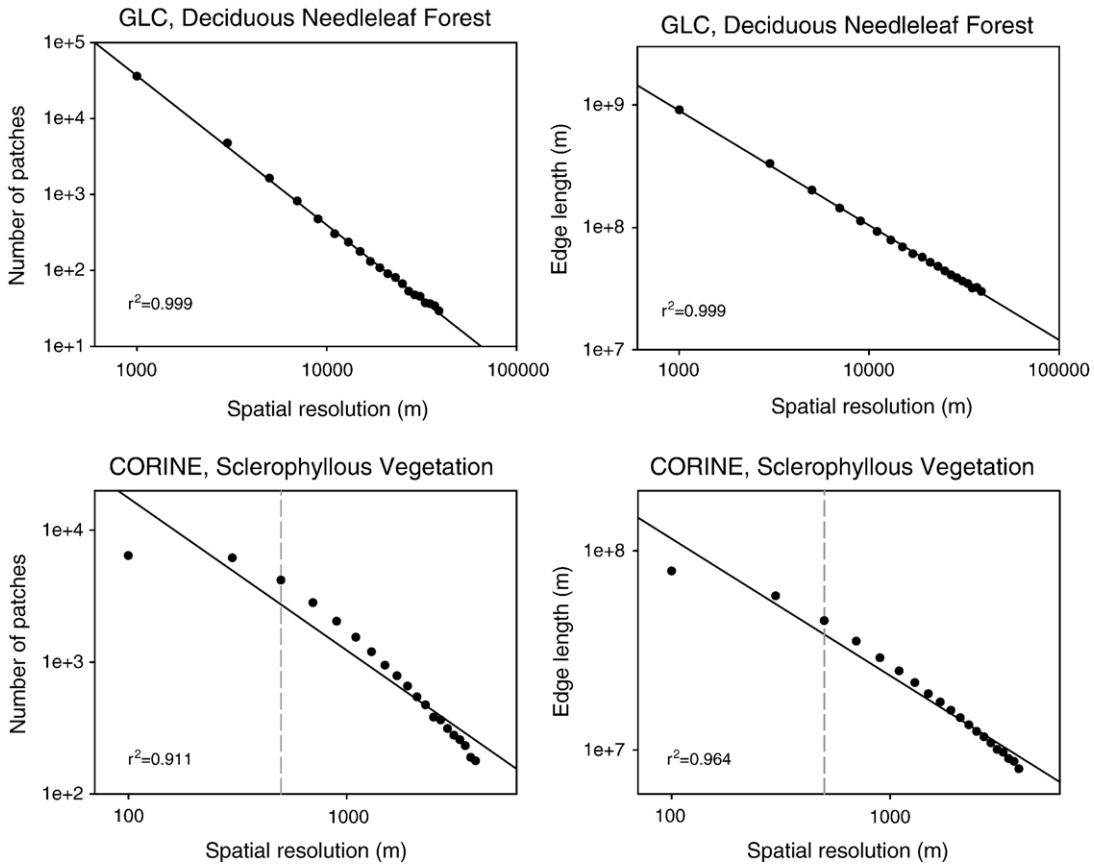

Fig. 4. Variation of two pattern metrics (NP and EL) as a function of spatial resolution in pixel-based data (GLC) and object-based data (CORINE) for two representative land cover classes (deciduous needleleaf forest and sclerophyllous vegetation, respectively). Previous studies have found power scaling functions to be the most appropriate for NP and EL, which would ideally result in NP and EL values (dots) following a perfect straight line in this double-log representation; the fitted power law (lines) and the resultant R^2 are included in each case. The dashed vertical lines in the CORINE plots correspond to the spatial resolution (500 m) equivalent to the MMU (25 ha) of this dataset. The scaling behaviour is similar for the other land cover classes and datasets with the same classification type.

is becoming more common in remote sensing for several reasons. First, much information is contained in the relationships between adjacent pixels, including texture, context and shape information, which allows the identification of individual objects as opposed to single pixels (Benz et al., 2004; Desclée et al., 2006; Hay et al., 2003; Laliberte et al., 2004; Walter, 2004). The easy integration of additional knowledge in object-oriented classifications is a valuable means to distinguish ecologically meaningful land cover types that do not have distinct spectral features, resulting in higher classification accuracies, particularly when high resolution images and heterogeneous land cover classes are involved (Bock et al., 2005; Desclée et al., 2006; Ehlers et al., 2003; Herold et al., 2002). On the other hand, ecologically speaking, it may be more appropriate to analyse objects as opposed to pixels because landscapes consist of patches that can be detected in the imagery with object-based analysis (Laliberte et al., 2004). The appearance of homogenous objects (rather than the per-pixel structure) is considered very valuable because it more likely relates to actual land use patterns in the landscape (Bock et al., 2005). Finally, land cover maps may not be accepted by end users when they show a "salt and pepper" appearance, as is often the case for pixel-based classifications (Bock et al., 2005). For these reasons, even when a map is obtained by means of per-pixel classifiers, post-classification processing techniques (such as majority filters, proximity functions, connectivity criteria) are often applied so that regions less than a present minimal area are removed (Davis and Peet, 1977; Homer et al., 1997; Imbernon and Branthomme, 2001; Kim, 1996; Saura, 2002). In any case, raster landscape data are distributed and available at pixel sizes below the final MMU, since this allows a better definition

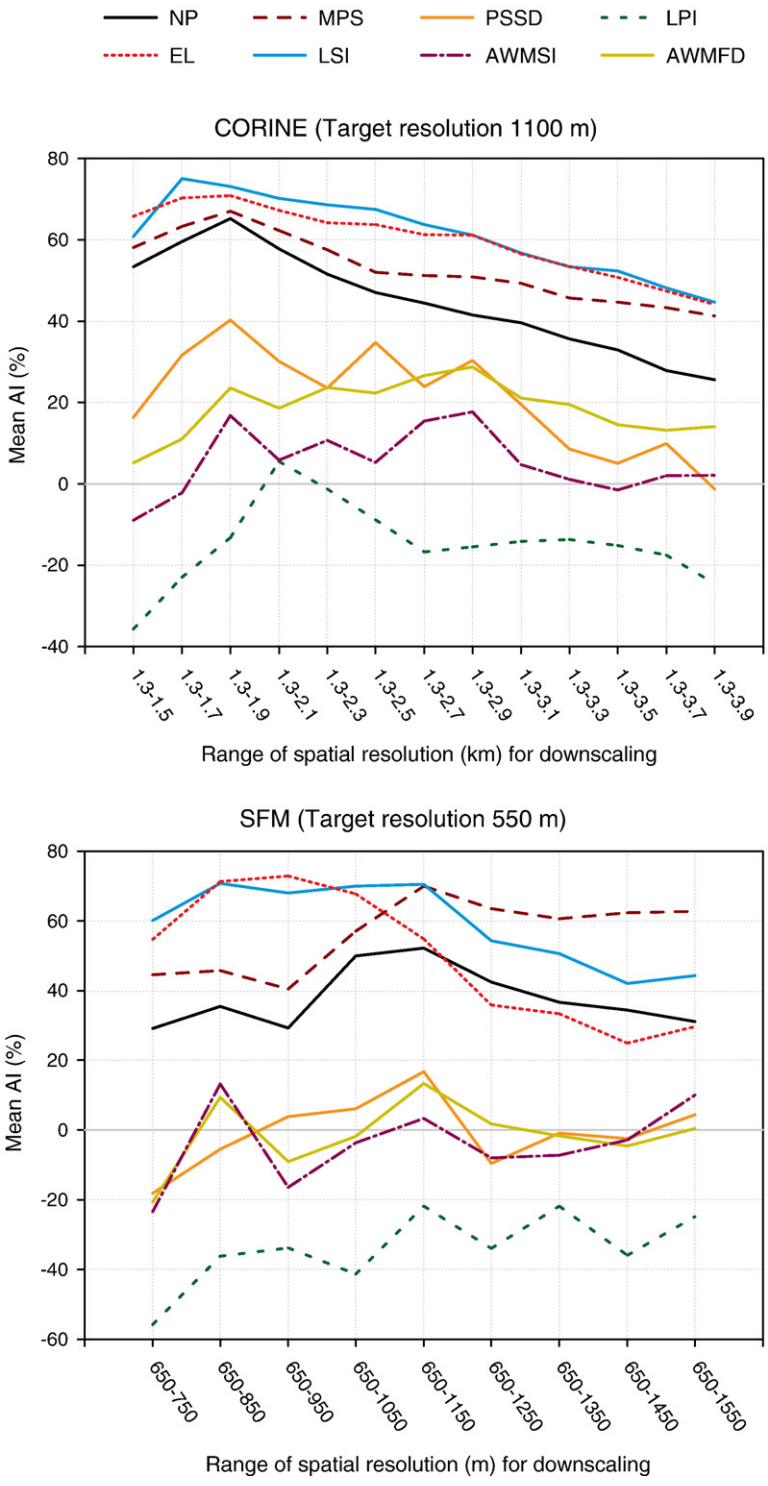

Fig. 5. Mean accuracy improvement (average of the AI values for the different land cover classes in each dataset) of the subpixel estimates for the different pattern metrics and ranges of spatial resolutions used to fit the scaling functions ("range of spatial resolution for downscaling"). Results are shown for the CORINE and SFM object-based datasets for a target resolution (1100 and 550 m respectively) above their minimum mapping unit (25 ha and 6.25 ha, respectively).

of patches boundaries with a subsequent benefit in terms of the spatial accuracy of the dataset.

3.2. Ranges of spatial resolution and downscaling factors

In the majority of the cases (83%) the highest AI for downscaling was obtained when only a few data points (values of the pattern metrics from two to six different spatial resolutions) were used to obtain the scaling function parameters and get the subpixel estimate at the target resolution (Figs. 2 and 5). Using only the two data points closest to the target resolution was the best downscaling procedure in many cases, especially for the pixel-based images (Fig. 2), while for the MMU images (with a target resolution above MMU, as noted in previous section) using about four to six data points tended to produce more accurate results (Fig. 5). This partially supports, with a much wider experimental basis, the results obtained by García-Gigorro and Saura (2005). They tried to estimate the values of NP, MPS and EL for a single forest class at 30 m of spatial resolution from scaling laws derived from an IRS-WiFS image (188 m, pixel-based classification). It was concluded that using only two data points provided the best result and that the "estimation errors resulted much larger as we considered additional spatial resolutions (coarser than 376 m and further apart from the target resolution of 30 m) for determining power law coefficients".

These results suggest that the scale behaviour of the pattern metrics (as described by available scaling functions) is not invariant across the full range of spatial resolutions. The rate of variation of the pattern metrics (as given by the scaling functions coefficients) estimated from a wide range of spatial resolutions diverges from the characteristic variation at subpixel resolutions. For this reason, using only a few metric values (those corresponding to the spatial resolutions closest to the target) produced the best results, compensating the fact that, at first glance, using fewer data points to fit the scaling functions may be considered less reliable from a statistical point of view.

As expected, the higher the downscaling factor (ratio between the finest available spatial resolution and the target spatial resolution, both measured as the length of a pixel side) the lower the accuracy of the resultant subpixel estimates (Fig. 6). This is a consequence of the fact that scaling functions do not perfectly replicate the variations of pattern metrics with spatial resolution, as noted earlier. Therefore, the extrapolation to increasingly finer pixel sizes has to be limited considering the true accuracy that these functions provide (Fig. 6). However, subpixel estimates were quite accurate in some cases even for considerably large downscaling factors: for example, in the GLC dataset, a downscaling factor equal to three resulted in AI of 88% for MPS and 61% for EL, and for a downscaling factor equal to 11 AI was 78% and 40%, respectively (Fig. 6).

3.3. Accuracy of the subpixel estimates for the different pattern metrics

For some metrics quite accurate subpixel estimates were achieved by using the scaling functions in all the datasets (for the best ranges of spatial resolution for obtaining the scaling laws parameters, as described in previous section). This is the case for MPS (AI about 70%–90% for all the datasets), LSI (AI about 65%–75%), and EL (AI about 60–70%) (Figs. 2 and 5). Scaling functions also proved useful for NP, achieving AI ranging from about 40% to 70%. However, scaling functions performed poorly for other metrics like LPI, for which a very low AI (even negative in most of the cases) was obtained (Figs. 2 and 5). For most of the metrics, there were no large differences between the average AI for the different datasets (Figs. 2 and 5). However, for the two shape metrics considered in this research (AWMSI and AWMFD) scaling functions performed much better in pixel-based images (GLC and NLC, achieving mean AI above 60%, Fig. 2) than in object-based images (CORINE and SFM, with the mean AI always below 25%, Fig. 5).

Even when all eight metrics have been previously reported as predictable in terms of their variations with spatial resolution (Type 1 class-level metrics in Wu (2004)), we found large differences in the accuracy of the subpixel estimates (in terms of AI) among pattern metrics (Figs. 2 and 5). Scaling functions have been described in the literature for all these metrics, but the actual performance of these functions seems to be highly variable depending on the metric. However, it is interesting to note that Wu (2004) differentiated two groups of predictable metrics: Type 1A and Type 1B in that study. Type 1A metrics (NP, LSI, EL) were those for which Wu (2004) obtained the most predictable behaviour, with scaling functions being consistent between the different analysed landscapes and between the different cover types within each landscape, while for Type 1B metrics (MPS, LPI, PSSD, AWMSI, AWMFD) a higher variability in the scaling behaviour between the different cover types within each landscape was detected. This is partially concordant with our analysis on downscaling accuracy; the three Type 1A metrics according to Wu (2004) were among the four most accurate in our study, but the best performing metric (MPS) in our subpixel estimates was considered as a Type 1B by Wu

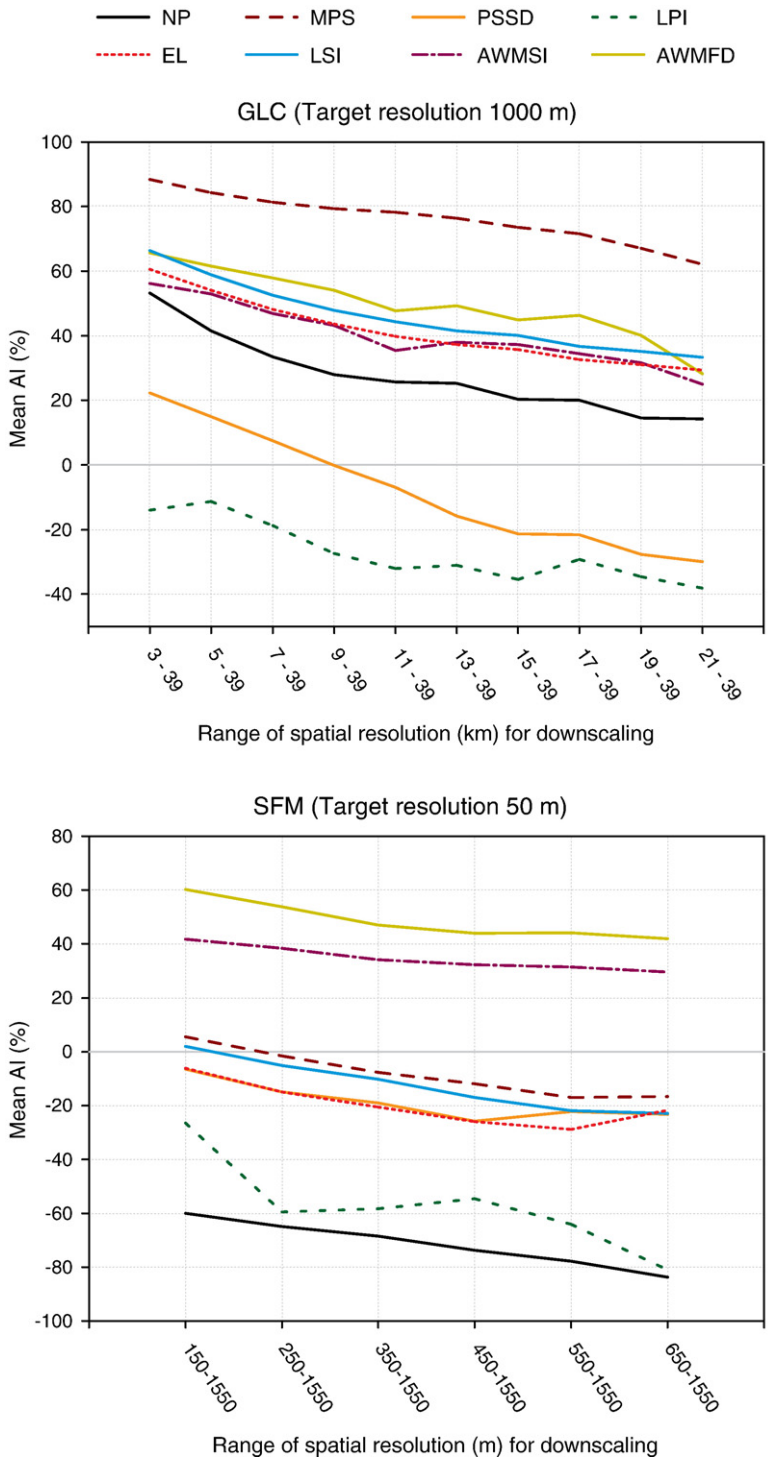

Fig. 6. Mean accuracy improvement (average of the AI values for the different land cover classes in each dataset) of the subpixel estimates for the GLC and SFM datasets and different downscaling factors (ranging from 3 to 21 for GLC and from 3 to 13 for SFM) for the different pattern metrics and a target resolution of 1 km (GLC) and 50 m (SFM). Similar results are obtained for the NLC and CORINE datasets. AI values are here computed maintaining in all cases the same value of the finest spatial resolution for downscaling within each dataset (Y_{fin}=3000 m for GLC and Y_{fin}=150 m for SFM, Eq. (4)) in order to render comparable the accuracies corresponding to different downscaling factors.

(2004). It should be noted that Wu (2004) did not provide any quantitative measure of the accuracy, predictability or goodness of fit of the different scaling functions and metrics types, which makes it difficult for further comparisons with our accuracy assessment. Frohn and Hao (2006) also concluded that LSI, NP and EL (these latter two measured as their equivalent patch density and edge density) were the most predictable with spatial resolution, which agrees with our results.

Wu (2004) suggested that the variability among cover types for Type 1B metrics may be caused by the low abundance of some patch types. However, in our data there was no strong effect from class abundance on resultant AI. For example, on GLC data a linear regression between class abundance and AI for the different metrics (using only two data points to obtain the scaling law parameters, which is the most adequate for this dataset, as shown in Fig. 2) yielded R^2 ranging only from 0.033 to 0.165. In fact, three of the four metrics with the highest R^2 were those classified as Type 1A (LSI, NP, EL), with R^2 about 0.150. Similar results were obtained for the other datasets. We further examined if other intrinsic characteristics of the analysed classes (different from class abundance) were responsible for the AI values we obtained. If that were the case, the same classes would present the highest AI for the different metrics. However, Spearman's correlations between the classes' AI values for the different metrics were not significant for any of the datasets, yielding only an average value of $r=0.269$. Therefore, the AI variability seems to be dependent on the predictability of the scaling behaviour of each particular metric and on the goodness of fit to the scaling variations of each function, rather than on intrinsic characteristics of land cover classes.

Very high determination coefficients (R^2) have been reported in previous research when fitting scaling functions to pattern metrics; for example R^2 above 0.96 has been obtained when fitting power functions through double-log linear regression (Frohn, 1998; Saura, 2004). This has been interpreted to mean that these metrics could be accurately extrapolated, transferred and compared across scales (e.g. Frohn, 1998; Wu et al., 2002). However, R^2 is not a good predictor of function performance, and the logarithmic transformation for fitting power laws through linear regression may underestimate the largest residuals and provide biased and inflated R^2 values (Heth et al., 1989; Saura, 2004). Indeed, we found that a high R^2 does not imply a good accuracy when downscaling through these functions. For example, for the sclerophyllous vegetation CORINE class and metrics in Fig. 4 we obtained a negative AI (as low as −93% for NP and −23% for EL when using only two data points for downscaling, which was the most accurate choice), despite that the R^2 values for the power laws were as high as $R^2=0.911$ for NP and $R^2=0.964$ for EL (Fig. 4). Apparently, R^2 values that are much higher than 0.95 are necessary to consider the power functions reliable for this purpose. For example, for the deciduous needleleaf forest GLC class (Fig. 4), with $R^2=0.999$ for the double-log fit, we obtained AI=52% for NP and AI=81% for EL (as before, when using only two data points for downscaling).

Our results do not fully support those obtained by García-Gigorro and Saura (2005) for a single forest class in central Spain, who reported high errors when estimating NP, EL and MPS values at 30 m of spatial resolution from power functions derived from an IRS-WiFS image (188 m) and concluded that these functions may not be really accurate or useful for downscaling fragmentation metrics. García-Gigorro and Saura (2005) also found in their data that NP presented a considerably lower accuracy than EL or MPS, and this is consistent with our results. They also concluded that further research on this scaling problem (with other spatial data and ranges of spatial resolution) was required, which has been addressed in this study. It is important to note that in some cases we found a high variability of the AI values for individual land cover classes, and therefore the results for a single class may diverge from the mean AI reported earlier (Figs. 2, 3 and 5). On average, the standard deviation of AI values for the different classes, metrics, and datasets was about 35%, being generally greater for those metrics, ranges of spatial resolutions and datasets with a poorer AI (Table 1). Standard deviations were

Table 1
Standard deviation of AI values for all the land cover classes in each of the datasets, for the target resolution and range of spatial resolution (range used to fit the scaling functions for downscaling) that provided the best results in each dataset

Pattern metric	GLC	NLC	CORINE	SFM
	Target: 1000 m	Target: 30 m	Target: 1100 m	Target: 550 m
	Range: 3000–5000 m	Range: 90–150 m	Range: 1300–1900 m	Range: 650–1150 m
NP	31.6	51.8	40.6	30.7
MPS	11.1	24.6	44.6	21.0
PSSD	27.3	35.7	42.4	55.5
LPI	55.3	51.0	49.8	61.6
EL	22.1	26.6	35.9	26.4
LSI	19.3	25.6	32.8	15.5
AWMSI	38.5	31.1	54.6	42.6
AWMFD	31.5	26.4	49.6	49.4

lower for the best performing metrics (MPS, LSI, EL), and higher for those metrics than provided less accurate subpixel estimates like LPI (Table 1). Standard deviations were also lower for the GLC dataset, where the highest AI was obtained (Fig. 2, Table 1).

4. Conclusions

We have shown that scaling functions are not perfect for downscaling landscape pattern metrics, but being aware of their limitations and the conditions necessary for their use, they can provide considerably accurate and useful subpixel estimates, even for relatively large downscaling factors. Previous studies, considering the apparent good statistical fit of scaling functions to metrics variations, have suggested that these functions may be used successfully for accurately scaling landscape pattern with no restrictions, in almost any circumstance. However, by performing an independent validation of the true accuracy of these scaling functions, we have shown that several important issues have to be taken into account in the future to avoid obtaining poor and potentially misleading results (even negative accuracy improvements) through their use. First, our results indicate that some of the metrics that have been considered thus far as predictable (in terms of their behaviour with spatial resolution) cannot be estimated accurately at finer resolutions, while for some others high accuracies can indeed be obtained (mean patch size, landscape shape index, edge length). Second, we suggest that only a few data points (those closest to the target resolution) should be used to fit the scaling functions, and not the full range of spatial resolutions that can be obtained through aggregation, since the rate of metric variation at increasingly broader scales diverges from the characteristic variation at subpixel resolutions. Third, we have shown that a good performance from available scaling functions may only be obtained for ranges of spatial resolutions above the minimum mapping unit fixed in the image segmentation or interpretation process. This applies to object-based classification of remotely sensed data, which is increasingly common due to the important advantages that this classification approach presents for landscape pattern analysis. Finally, it should be noted that our results have been obtained for those metrics for which a predictable scaling behaviour had been reported in previous studies. Other pattern metrics may present erratic variations with spatial resolution and, therefore, would provide much poorer subpixel estimates, since for them no reliable or consistent scaling function has been found (Wu, 2004).

It is important to note that downscaling through scaling functions does not require any prior information on pattern characteristics at the subpixel level, which makes it a very attractive procedure. It also provides an overall subpixel metric value for each of the land cover classes, but not the spatial pattern itself nor the location of specific land cover classes in individual pixels. Therefore, this is different from the approach for mapping subpixel land cover spatial patterns by Tatem et al. (2002), which is based on a Hopfield neural network and requires prior information on land cover pattern (quantified through semivariance values in that study) at the target resolution, providing multiple, equally probable land cover distributions that accommodate input semivariance values (Tatem et al., 2002). An interesting topic for further research is the possible integration of both approaches, so that scaling functions estimate subpixel pattern characteristics as quantified by different metrics (therefore avoiding the need for prior information on subpixel pattern, which may be quite difficult to have in practical applications) and the Hopfield neural network approach provides subpixel spatial patterns in accordance with those downscaled metric values.

We believe that our results and recommendations provide relevant insights into this important scaling problem, in a context where satellite images with different spatial resolutions are increasingly being used for the analysis of landscape pattern, which represents a key variable to better understand and characterise many ecological and environmental processes.

Acknowledgements

Funding was provided by the Ministerio de Educación y Ciencia (Spain) and the European Union (FEDER funds) through CONEFOR (REN2003-01628) and IBEPFOR (CGL2006-00312/BOS) projects. The Spanish Forest Map was provided by the Dirección General para la Biodiversidad (Ministerio de Medio Ambiente, Spain). Special thanks to Begoña de la Fuente Martín for her valuable assistance in this research. Two anonymous reviewers made helpful comments on an earlier version of this manuscript.

References

Benson, B.J., MacKenzie, M.D., 1995. Effects of sensor spatial resolution on landscape structure parameters. Landscape Ecology 10 (2), 113–120.

Benz, U.C., Hofmann, P., Willhauck, G., Lingenfelder, I., Heynen, M., 2004. Multi-resolution, object-oriented fuzzy analysis of remote sensing data for GIS-ready information. ISPRS Journal of Photogrammetry and Remote Sensing 58 (3–4), 239–258.

Betts, M.G., Franklin, S.E., Taylor, R.G., 2003. Interpretation of landscape pattern and habitat change for local indicator species using satellite imagery and geographic information system data in

New Brunswick, Canada. Canadian Journal of Forest Research 33 (10), 1821–1831.

Bock, M., Rossner, G., Wissen, M., Remm, K., Langanke, T., Lang, S., Klug, H., Blaschke, T., Vrscaj, B., 2005. Spatial indicators for nature conservation from European to local scale. Ecological Indicators 5 (4), 322–338.

Colombo, S., Chica-Olmo, M., Abarca, F., Eva, H., 2004. Variographic analysis of tropical forest cover from multi-scale remotely sensed imagery. ISPRS Journal of Photogrammetry and Remote Sensing 58 (5–6), 330–341.

Commission of the European Communities, 1993. CORINE Land Cover: Guide Technique, Report EUR 12585 EN. Office for Publications of the European Communities, Luxembourg.

Davis, W.A., Peet, F.G., 1977. A method of smoothing digital thematic maps. Remote Sensing of Environment 6 (1), 45–49.

Desclée, B., Bogaert, P., Defourny, P., 2006. Forest change detection by statistical object-based method. Remote Sensing of Environment 102 (1–2), 1–11.

Egbert, S.L., Park, S., Price, K.P., Lee, R.Y., Wu, J., Nellis, M.D., 2002. Using conservation reserve program maps derived from satellite imagery to characterize landscape structure. Computers and Electronics in Agriculture 37 (1–3), 141–156.

Ehlers, M., Gähler, M., Janowsky, R., 2003. Automated analysis of ultra high resolution remote sensing data for biotope type mapping: new possibilities and challenges. ISPRS Journal of Photogrammetry and Remote Sensing 57 (5–6), 315–326.

Forman, R.T.T., 1995. Land Mosaics: the Ecology of Landscapes and Regions. Cambridge University Press, Cambridge, United Kingdom.

Frohn, R.C., 1998. Remote Sensing for Landscape Ecology: New Metric Indicators for Monitoring, Modeling and Assessment of Ecosystems. CRC-Lewis Publishers, Boca Raton, Florida, USA.

Frohn, R.C., Hao, Y., 2006. Landscape metric performance in analyzing two decades of deforestation in the Amazon Basin of Rondonia, Brazil. Remote Sensing of Environment 100 (2), 237–251.

Frohn, R.C., McGwire, K.C., Dale, V.H., Estes, J.E., 1996. Using satellite remote sensing analysis to evaluate a socio-economic and ecological model of deforestation in Rondonia, Brazil. International Journal of Remote Sensing 17 (16), 3233–3255.

García-Gigorro, S., Saura, S., 2005. Forest fragmentation estimated from remotely sensed data: is comparison across scales possible? Forest Science 51 (1), 51–63.

Griffith, J.A., Stehman, S.V., Sohl, T.L., Loveland, T.R., 2003. Detecting trends in landscape pattern metrics over a 20-year period using a sampling-based monitoring programme. International Journal of Remote Sensing 24 (1), 175–181.

Hansen, M.J., Franklin, S.E., Woudsma, C.G., Peterson, M., 2001. Caribou habitat mapping and fragmentation analysis using Landsat MSS, TM, and GIS data in the North Columbia Mountains, British Columbia, Canada. Remote Sensing of Environment 77 (1), 50–65.

Hay, G.J., Blaschke, T., Marceasu, D.J., Bouchard, A., 2003. A comparison of three image–object methods for the multiscale analysis of landscape structure. ISPRS Journal of Photogrammetry and Remote Sensing 57 (5–6), 327–345.

He, H.S., DeZonia, B.E., Mladenoff, D.J., 2000. An aggregation index (AI) to quantify spatial patterns of landscapes. Landscape Ecology 15 (7), 591–601.

Herold, M., Scepan, J., Clarke, K.C., 2002. The use of remote sensing and landscape metrics to describe structures and changes in urban land uses. Environment and Planning A 34 (8), 1443–1458.

Heth, C.D., Pierce, W.D., Belke, T.W., Hensch, S.A., 1989. The effect of logarithmic transformation on estimating the parameters of the generalized matching law. Journal of the Experimental Analysis of Behavior 52 (1), 65–76.

Hlavka, C.A., Livingston, G.P., 1997. Statistical models of fragmented land cover and the effect of coarse spatial resolution on the estimation of area with satellite sensor imagery. International Journal of Remote Sensing 18 (10), 2253–2259.

Homer, C.G., Ramsey, R.D., Edwards, T.C., Falconer, A., 1997. Landscape cover type modeling using a multi-scene thematic mapper mosaic. Photogrammetric Engineering and Remote Sensing 63 (1), 59–67.

Imbernon, J., Branthomme, A., 2001. Characterization of landscape patterns of deforestation in tropical rain forests. International Journal of Remote Sensing 22 (9), 1753–1765.

Jorge, L.A.B., García, G.J., 1997. A study of habitat fragmentation in Southeastern Brazil using remote sensing and geographic information systems (GIS). Forest Ecology and Management 98 (1), 35–47.

Kim, K.E., 1996. Adaptive majority filtering for contextual classification of remote sensing data. International Journal of Remote Sensing 17 (5), 1083–1087.

Kojima, N., Laba, M., Velez-Liendo, X.M., Bradley, A.V., Millington, A.C., Baveye, P., 2006. Causes of the apparent scale independence of fractal indices associated with forest fragmentation in Bolivia. ISPRS Journal of Photogrammetry and Remote Sensing 61 (2), 84–94.

Laliberte, A.S., Rango, A., Havstad, K.M., Paris, J.F., Beck, R.F., McNeely, R., Gonzalez, A.L., 2004. Object-oriented image analysis for mapping shrub encroachment from 1937 to 2003 in southern New Mexico. Remote Sensing of Environment 93 (1–2), 198–210.

Loveland, T.R., Reed, B.C., Brown, J.F., Ohlen, D.O., Zhu, Z., Yang, L., Merchant, J.W., 2000. Development of a global land cover characteristics database and IGBP DISCover from 1 km AVHRR data. International Journal of Remote Sensing 21 (6–7), 1303–1330.

McGarigal, K., Cushman, S.A., Neel, M.C., Ene, E., 2002. Fragstats: Spatial Pattern Analysis Program for Categorical Maps. University of Massachusetts, Amherst. http://www.umass.edu/landeco/research/fragstats/fragstats.html (accessed March 7, 2007).

Millington, A.C., Velez-Liendo, X.M., Bradley, A.V., 2003. Scale dependence in multitemporal mapping of forest fragmentation in Bolivia: implications for explaining temporal trends in landscape ecology and applications to biodiversity conservation. ISPRS Journal of Photogrammetry and Remote Sensing 57 (4), 289–299.

Ministerio de Medio Ambiente, 2002. Tercer Inventario Forestal Nacional, Murcia. Dirección General de Conservación de la Naturaleza, Madrid, Spain.

Pal, N.R., Pal, S.K., 1993. A review on image segmentation techniques. Pattern Recognition 26 (9), 1277–1294.

Peralta, P., Mather, P., 2000. An analysis of deforestation patterns in the extractive reserves of Acre, Amazonia from satellite imagery: a landscape ecological approach. International Journal of Remote Sensing 21 (13–14), 2555–2570.

Sachs, D.L., Sollins, P., Cohen, W.B., 1998. Detecting landscape changes in the interior of British Columbia from 1975 to 1992 using satellite imagery. Canadian Journal of Forest Research 28 (1), 23–36.

Sader, S.A., Bertrand, M., Wilson, E.H., 2003. Satellite change detection of forest harvest patterns on an industrial forest landscape. Forest Science 49 (3), 341–353.

Saura, S., 2001. Influencia de la Escala en la Configuración del Paisaje: Estudio Mediante un Nuevo Método de Simulación Espacial, Imágenes de Satélite y Cartografías Temáticas. Ph. D. Thesis, Department of Forest Economics and Management, Universidad Politécnica de Madrid, Spain.

Saura, S., 2002. Effects of minimum mapping unit on land cover data spatial configuration and composition. International Journal of Remote Sensing 23 (22), 4853–4880.

Saura, S., 2004. Effects of remote sensor spatial resolution and data aggregation on selected fragmentation indices. Landscape Ecology 19 (2), 197–209.

Saura, S., Carballal, P., 2004. Discrimination of native and exotic forest patterns through shape irregularity indices: an analysis in the landscapes of Galicia, Spain. Landscape Ecology 19 (6), 647–662.

Saura, S., Martínez-Millán, J., 2001. Sensitivity of landscape pattern metrics to map spatial extent. Photogrammetric Engineering and Remote Sensing 67 (9), 1027–1036.

Skole, D.L., Tucker, C.J., 1993. Tropical deforestation and habitat fragmentation in the Amazon: satellite data from 1978 to 1988. Science 260 (5116), 1905–1910.

Tatem, A.J., Lewis, H.G., Atkinson, P.M., Nixon, M.S., 2002. Super-resolution land cover pattern prediction using a Hopfield neural network. Remote Sensing of Environment 79 (1), 1–14.

Turner, M.G., 1989. Landscape ecology: the effect of pattern on process. Annual Review of Ecology and Systematics 20, 171–197.

Turner, M.G., O'Neill, R.V., Gardner, R.H., Milne, B.T., 1989. Effects of changing spatial scale on the analysis of landscape pattern. Landscape Ecology 3 (3–4), 153–162.

Vogelmann, J.E., 1995. Assessment of forest fragmentation in Southern New England using remote sensing and geographic information systems technology. Conservation Biology 9 (2), 439–449.

Vogelmann, J.E., Sohl, T., Howard, S.M., 1998a. Regional characterization of land cover using multiple sources of data. Photogrammetric Engineering and Remote Sensing 64 (1), 45–57.

Vogelmann, J.E., Sohl, T., Campbell, P.V., Shaw, D.M., 1998b. Regional land cover characterization using Landsat Thematic Mapper data and ancillary data sources. Environmental Monitoring and Assessment 51 (1–2), 415–428.

Walter, V., 2004. Object-based classification of remote sensing data for change detection. ISPRS Journal of Photogrammetry and Remote Sensing 58 (3–4), 225–238.

Wickham, J.D., Riitters, K.H., 1995. Sensitivity of landscape metrics to pixel size. International Journal of Remote Sensing 16 (18), 3585–3594.

Wu, J., 2004. Effects of changing scale on landscape pattern analysis: scaling relations. Landscape Ecology 19 (2), 125–138.

Wu, J., Jelinski, D.E., Luck, M., Tueller, P.T., 2000. Multiscale analysis of landscape heterogeneity: scale variance and pattern metrics. Geographic Information Sciences 6 (1), 6–19.

Wu, J., Shen, W., Sun, W., Tueller, P.T., 2002. Empirical patterns of the effects of changing scale on landscape metrics. Landscape Ecology 17 (8), 761–782.

Yu, X., Ng, C., 2006. An integrated evaluation of landscape change using remote sensing and landscape metrics: a case study of Panyu, Guangzhou. International Journal of Remote Sensing 27 (6), 1075–1092.